Magnetic field and temperature dependence of the amplitude-modulated magnetic structure of PrNi2Si2 determined by single-crystal neutron diffraction

J. A. Blanco, B. Fåk, E. Ressouche, B. Grenier, M. Rotter, D. Schmitt, J. A. Rodríguez-Velamazán, J. Campo, Pascal Lejay

Magnetic field and temperature dependence of the amplitude-modulated magnetic structure of $PrNi_2Si_2$ determined by single-crystal neutron diffraction

J. A. Blanco,[1] B. Fåk,[2] E. Ressouche,[2] B. Grenier,[2,3] M. Rotter,[4] D. Schmitt,[5] J. A. Rodríguez-Velamazán,[6,7] J. Campo,[7] and P. Lejay[8]

[1]*Departamento de Física, Universidad de Oviedo, E-33007 Oviedo, Spain*
[2]*Commissariat à l'Energie Atomique, INAC, SPSMS, 38054 Grenoble, France*
[3]*Université Joseph Fourier, Grenoble-I, France*
[4]*Department of Physics, Clarendon Laboratory, University of Oxford, Parks Road, Oxford OX1 3PU, United Kingdom*
[5]*Laboratoire de Géophysique Interne et Tectonophysique (LGIT), CNRS-UJF, BP 53, 38041 Grenoble Cedex 9, France*
[6]*Institut Laue Langevin, 6 rue Jules Horowitz, BP 156, 38042 Grenoble Cédex 9, France*
[7]*Instituto de Ciencia de Materiales de Aragón, CSIC–Universidad de Zaragoza, 50009 Zaragoza, Spain*
[8]*Institut Néel, CNRS, BP 166, 38042 Grenoble Cedex 9, France*

(Received 15 January 2010; revised manuscript received 30 April 2010; published 11 August 2010)

The temperature and magnetic field dependence of the magnetic structure in the singlet crystal-field ground-state system $PrNi_2Si_2$ have been determined using single-crystal neutron diffraction. At the magnetic ordering temperature in zero field, $T_N=20.0\pm0.5$ K, an amplitude-modulated magnetic structure sets in with a propagation vector $\mathbf{k}=(0,0,0.87)$ and the magnetic moments of the Pr^{3+} ions parallel to the c axis of the body-centered tetragonal structure. The magnetic structure remains amplitude modulated down to low temperatures ($T=1.6$ K) with only a small tendency to squaring up, as signaled by the weak intensity of the third harmonic that develops below 16 K. With applied field along the easy axis, the modulated structure goes smoothly over into a ferromagnetic state. At the critical field of $H_c=58$ kOe, the first harmonic disappears and the field-induced ferromagnetic moment shows a kink, in agreement with magnetization measurements. Both the temperature and magnetic field dependence are well described by a periodic field Hamiltonian including magnetic exchange and the crystalline electric field.

DOI: 10.1103/PhysRevB.82.054414 PACS number(s): 75.25.−j, 75.10.Dg, 75.50.Ee, 61.05.fg

I. INTRODUCTION

Frustration in magnetic systems occurs when the interaction energies cannot be simultaneously minimized.[1–3] This may arise from the topology of the lattice (geometric frustration) or from competing magnetic interactions. Magnetic frustration leads often to complex magnetic structures—e.g., incommensurate, noncollinear, or amplitude-modulated—or ground states that are not magnetically ordered, such as spin glasses, spin liquids, and nematic order. In rare earth-based intermetallic compounds,[4,5] the long-range and oscillatory character of the Ruderman-Kittel-Kasuya-Yosida (RKKY) interaction lead to a maximum of the Fourier transform of the exchange interactions, $J(\mathbf{q})$, for a wave vector $\mathbf{q}$ that may be not commensurate with the reciprocal lattice, resulting in incommensurate magnetic structures. If the system has a strong easy-axis anisotropy due to crystal field effects, the resulting magnetic structure may be amplitude modulated, i.e., the size of the ordered magnetic moment varies from one site to the next. In general, such magnetic structures are not stable down to zero temperature since it is not entropically favorable for a doublet ground state to have zero ordered magnetic moment on some of the sites. Amplitude-modulated structures are therefore often stable only just below the magnetic transition temperature, T_N. At lower temperatures, the system *either* evolves into a magnetic structure with equal size of the moments, a so-called "squaring up" characterized by the appearance of higher order harmonics $(3\mathbf{k},5\mathbf{k},\ldots)$ of the propagation vector $\mathbf{k}$, *or* undergoes a transition to a commensurate magnetic structure.[6]

In the case of a singlet ground-state system, where the ordered magnetic moment is induced by a coupling to an excited state via the RKKY interaction, an amplitude-modulated structure may persist down to zero temperature. There are few examples in the literature of systems exhibiting this type of magnetic ordering (such as chromium[7] and erbium[8] metals or phosphorous-rich $Eu(As_{1-x}P_x)_3$ compounds[9]) and they are often model systems where quantitative analysis can be performed allowing an accurate determination of the relevant interactions. Of particular interest in this context is $PrNi_2Si_2$.[10–16] It has a strong easy-axis anisotropy with a ratio $\chi_c/\chi_a\approx4.5$ of the magnetic susceptibility above the ordering temperature and displays an amplitude-modulated magnetic structure below $T_N=20$ K.[10]

In order to confirm that the magnetic structure of $PrNi_2Si_2$ remains amplitude-modulated down to low temperatures, we have performed new single-crystal neutron-diffraction measurements. The high precision in these measurements allow us to quantitatively determine the first and third harmonics as a function of temperature. In this way, we have measured the magnetic field dependence of the magnetic structure with $H\|c$ in order to test predictions of model calculations.[12,13]

II. EXPERIMENTAL

$PrNi_2Si_2$ crystallizes in the body-centered tetragonal $ThCr_2Si_2$-type structure with space group $I4/mmm$ (No. 139) and lattice parameters $a=4.047$ and $c=9.621$ Å.[10] The Pr atoms are in the position 2a at (0,0,0) with point symmetry $4/mmm$, Ni is located at the 4d position at (0,1/2,1/4) and

(1/2,0,1/4), while the Si is on the 4e position at $(0,0,\pm z)$.

Several single crystals of $PrNi_2Si_2$ were grown using the Czochralski method with starting materials of at least 99.99% purity. These crystals were mounted with the c-axis vertical and studied using the D15 and D23 neutron diffractometers at the high-flux reactor of the Institut Laue-Langevin (Grenoble, France).

The nuclear structure was determined at $T=40$ K on a small single crystal of volume 0.8 mm^3 using the D23 lifting-arm diffractometer with a neutron wavelength of $\lambda=1.2789$ Å from a Cu(200) monochromator. In total, 330 reflections were collected and corrected for absorption and extinction effects. The measurements confirm the crystal structure and a least square-refinement gave $z=0.3712(4)$ with a goodness of fit of $R_B=5.0\%$. Measurements at $T=2$ K show that the nuclear structure remains the same in the magnetically ordered phase.

The magnetic structure was studied in zero field using the same small crystal on D23 with $\lambda=2.3782$ Å from a PG(002) monochromator. Higher order contamination was eliminated by the use of a graphite filter in the incoming beam. The positions of the magnetic satellites were determined from scans of the wave vector **Q** along the Q_z direction while rocking scans were used to determine the integrated intensities.

A larger crystal of volume 30 mm^3 was used to study the magnetic structure at low temperatures, $T<3.2$ K with a magnetic field up to 110 kOe applied along the tetragonal c axis. The measurements were made under field-cooled conditions, i.e., all field changes were made in the paramagnetic phase. D23 was used with $\lambda=1.2815$ Å from a Cu(200) monochromator.

III. RESULTS

Our single-crystal neutron-diffraction measurements clearly establish that the magnetic propagation vector is $\mathbf{k}=(0,0,0.870)$, in agreement with earlier powder neutron diffraction results.[10] In addition, the higher sensitivity allowed us to observe the third harmonic $3\mathbf{k}$ at low temperatures (see Fig. 1) but not the fifth harmonic. The absence of magnetic reflections for **Q** along the c^* axis implies that the Pr^{3+} magnetic moments are oriented along the c direction, in agreement with the easy-axis anisotropy revealed by magnetic susceptibility measurements.[10] This is also in accordance with representation analysis, applicable to second-order phase transitions: symmetry allows the moments to be either along the c axis *or* (anywhere) in the basal *ab* plane. The constraints between the components of Fourier coefficients describing the possible magnetic structures can be found in Table I.

The magnetic structure was refined using 94 magnetic Bragg reflections with a reliability factor of $R_B=8.8\%$ (see Fig. 2). In the refinements the moments at the Ni and Pr sites were allowed to vary independently, both along c and in the *ab* plane, with the symmetry-imposed constraints listed in Table I. The fits converged to a solution where only Pr sites were ordered, with moments along the c direction, corresponding to the Γ_2 irreducible representation in Table I. No magnetic moment was found on the Ni sites, to an experimental precision of $\pm 0.05\ \mu_B$. These results are similar to related RNi_2Si_2 compounds.[5] We used the Pr^{3+} magnetic form factor from Ref. 17. Going beyond the dipole approximation[18] using the known crystal field parameters of $PrNi_2Si_2$ changes the form factor by at most 3% for $Q<20$ $Å^{-1}$. At $T=1.6$ K, the first and third Fourier components of the Pr^{3+} magnetic moments were $M_{\mathbf{k}}=2.35\pm0.02\ \mu_B$ and $M_{3\mathbf{k}}=0.34\pm0.19\ \mu_B$, respectively. The former value is quite close to the value found by powder neutron diffraction, 2.6 μ_B (Fig. 3).[10]

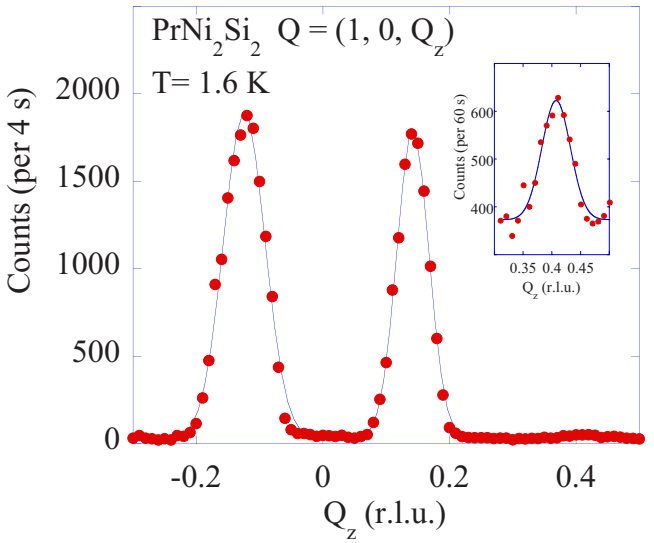

FIG. 1. (Color online) Scan along the line $\mathbf{Q}=(1,0,Q_z)$ at $T=1.6$ K showing the peaks related to the first harmonic $\mathbf{k}=(0,0,0.87)$ of the amplitude-modulated magnetic structure of $PrNi_2Si_2$, which occurs here at $Q_z=\pm0.13$ due to the body centering. The inset shows the peak related to the third harmonic, $3\mathbf{k}=(0,0,0.61)$. The lines are Gaussian fits.

The temperature dependence of the Fourier components of the magnetic moment (first and third harmonics) as obtained from the integrated neutron intensities are shown in Fig. 4. The Néel temperature obtained from the first harmonic is $T_N=20.0\pm0.5$ K. No change in the incommensurate propagation vector was observed with temperature. The third harmonic is only observed below 16 K. The temperature dependence of the ratio of the two harmonics, $M_{3\mathbf{k}}/M_{\mathbf{k}}$, is shown in the inset of Fig. 4. At the lowest temperature

TABLE I. Symmetry-allowed Fourier components of the magnetic moment constructed from linear combinations of the basis vectors corresponding to the irreducible representations (IREP) for space group $I4/mmm$ with propagation vector $\mathbf{k}=(0,0,0.87)$. There is one Pr atom per primitive unit cell at the Wyckoff site 2a and two Ni atoms at site 4d. The coefficients u, v, r, s, w, and p can be complex.

IREP	2a Pr(0,0,0)	4d Ni(0,0.5,0.25)	4d Ni(0.5,0,0.25)
Γ_2	$(0,0,u)$	$(0,0,r)$	$(0,0,r)$
Γ_4		$(0,0,r)$	$(0,0,-r)$
Γ_5	$(u,iv,0)$	$(r,s,0)$	$i(w,p,0)$

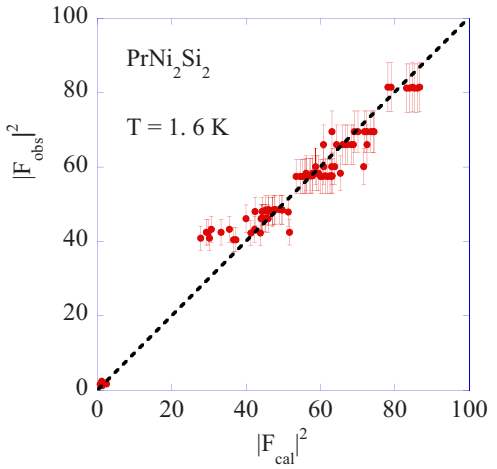

FIG. 2. (Color online) Observed and calculated square modulus of the structure factor obtained from the magnetic refinement of the present single-crystal neutron-diffraction data collected at $T=1.6$ K. The calculated structure factor corresponds to the amplitude–modulated magnetic structure of $PrNi_2Si_2$ (see text).

measured, $T=1.6$ K, the Fourier component of the third harmonic is $\sim 1/7$ of that of the first harmonic. This implies that the magnetic structure remains close to sinusoidal even at the lowest temperatures, far from the equal-amplitude "squared-up" structure, where the ratio is 1/3.

The magnetic field dependence of both the first and the third harmonics was determined from scans along the Q_z direction at $\mathbf{Q}=(1,0,Q_z)$, see Fig. 5. Within the experimental precision, neither the peak width nor the peak position of the first harmonic is affected by the applied field. The integrated intensities were obtained from fits to Gaussian functions, from which the field dependence of the Fourier component of the first harmonic, $M_{\mathbf{k}}$, was extracted, see Fig. 6(a). Figure 5 shows that the third harmonic, $M_{3\mathbf{k}}$, disappears more quickly with field than does the first harmonic, but the weak intensity precludes a detailed analysis of its field dependence.

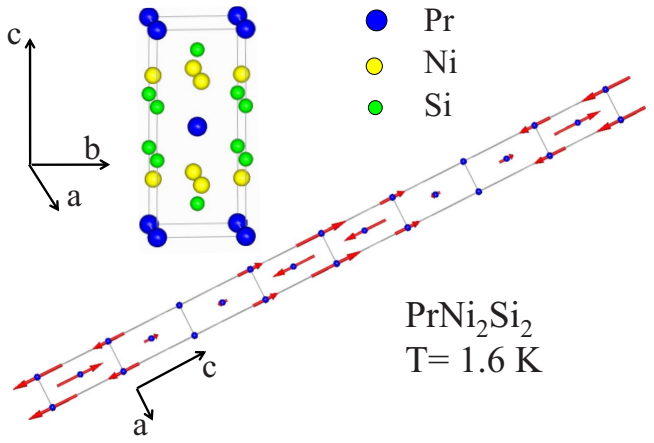

FIG. 3. (Color online) Projection of the amplitude-modulated magnetic structure of $PrNi_2Si_2$ on the ac plane of the body-centered tetragonal unit cell, determined from the present single-crystal neutron-diffraction data at $T=1.6$ K. The unit cell of the crystallographic structure is also shown.

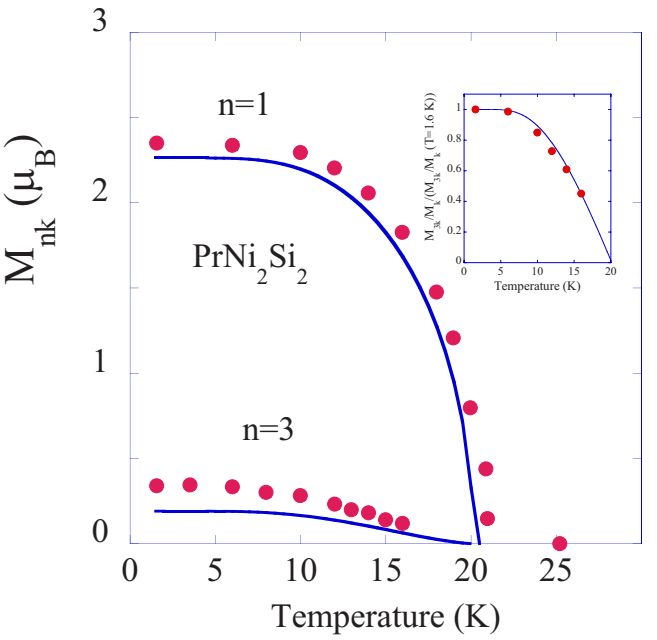

FIG. 4. (Color online) Temperature dependence of the Fourier components $M_{\mathbf{k}}$ and $M_{3\mathbf{k}}$ of the amplitude-modulated magnetic structure of $PrNi_2Si_2$. Symbols are present experimental results while lines are values calculated from the periodic field model. The inset shows the experimental and calculated ratio $M_{3\mathbf{k}}/M_{\mathbf{k}}$ scaled to agree at the lowest temperature.

The magnetic field induces a ferromagnetic component, which was determined from rocking scans of weak nuclear Bragg peaks, such as the (011) reflection. The field dependence of strong nuclear Bragg peaks, such as (020), was found to be negligible, indicating that the extinction is not affected by the applied field. The so-determined ferromagnetic Fourier component M_0 induced by the magnetic field is shown in Fig. 6(b). The results are very similar to that of the measured bulk magnetization.[12,13]

IV. ANALYSIS

The magnetism of Pr^{3+} can be understood from its Hund's rule ground state $^3H_4$ with total angular momentum $J=4$, the next multiplet state being ~ 3000 K higher in energy.[19] Under the influence of a tetragonal crystal field (point group D_{4h}, quantization axis c), with Hamiltonian

$$\mathcal{H}_{\mathrm{CEF}} = B_2^0 O_2^0 + B_4^0 O_4^0 + B_4^4 O_4^4 + B_6^0 O_6^0 + B_6^4 O_6^4, \qquad (1)$$

where O_l^m and B_l^m are the Stevens operators and crystal-field parameters, respectively,[20] the ninefold degenerate Hund's rule ground state is split into five singlets and two doublets.[21] A joint analysis of specific heat, magnetization, magnetic susceptibility, and inelastic neutron-scattering measurements suggests a singlet crystal-field ground state[12,13]

$$\Gamma_1^{(1)} = \sin\beta_1 \frac{|4\rangle + |-4\rangle}{\sqrt{2}} - \cos\beta_1 |0\rangle,$$

which is responsible for the easy-axis anisotropy. The first excited state is a singlet at an energy of 38 K

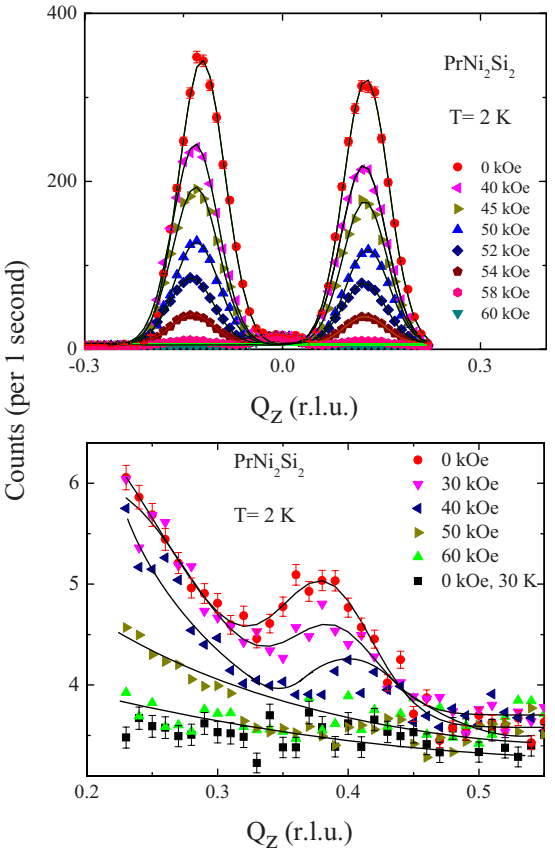

FIG. 5. (Color online) Scans along Q_z at $\mathbf{Q}=(1,0,Q_z)$ and $T=2$ K of the first (upper panel) and third (lower panel) harmonics for different magnetic fields $H\|c$. Note that the third harmonic is much weaker than the first harmonic. The lines are Gaussian fits plus a background.

$$\Gamma_2 = \frac{|4\rangle - |-4\rangle}{\sqrt{2}}$$

and the second excited state is a doublet at 58 K

$$\Gamma_5^{(1)} = \sin\beta_2|\pm 3\rangle - \cos\beta_2|\mp 1\rangle,$$

where $\beta_1=2.159$ and $\beta_2=1.820$ are constants defined in Ref. 21 and determined in Refs. 12 and 13.

The ordered magnetic moment in $PrNi_2Si_2$ is induced by the RKKY exchange interaction, which mixes the two lowest lying crystal field singlets. We model this by combining the crystal-field Hamiltonian (1) with an N-site mean-field approximation of the exchange interactions $\Sigma_{i,j}J_{i,j}\mathbf{M}(i)\cdot\mathbf{M}(j)$, where $\mathbf{M}(j)$ is the ordered magnetic moment of site j. This leads to the so-called self-consistent periodic field model[12,13]

$$\mathcal{H} = \sum_{j=1}^{N}\mathcal{H}_{\mathrm{CEF}}(j) - \sum_{j=1}^{N}\mathbf{H}\cdot\mathbf{M}(j) - \sum_{j=1}^{N}\mathbf{H}_{\mathrm{ex}}(j)\cdot\mathbf{M}(j) + \frac{1}{2}\sum_{j=1}^{N}\langle\mathbf{M}(j)\rangle\cdot\mathbf{H}_{ex}(j), \qquad (2)$$

where N is the number of magnetic ions over one period of the magnetic structure. The second term in Eq. (2) represents

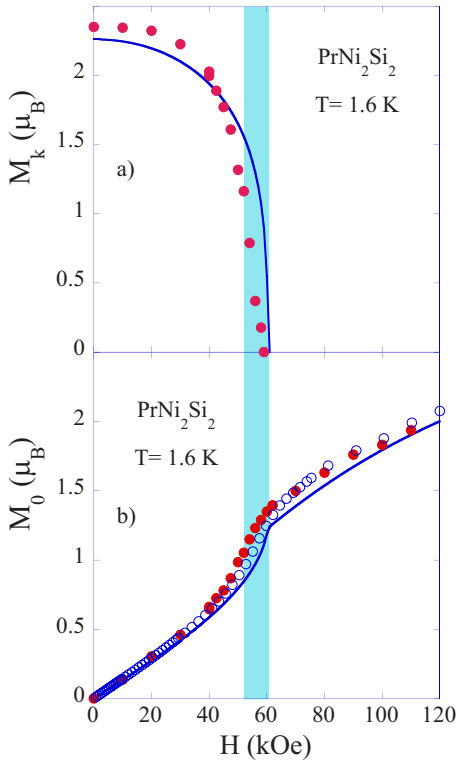

FIG. 6. (Color online) Magnetic field dependence (a) of the first Fourier component $M_{\mathbf{k}}$ and (b) of the ferromagnetic Fourier component M_0 for $H\|c$. The red solid circles are from the present diffraction data while the blue open circles in (b) are from magnetization measurements (Refs. 12 and 13). The solid lines correspond to the periodic field model. The blue shadowed area represents the region where $0<M_{\mathbf{k}}<M_0$ (see the text for more details).

the Zeeman coupling of the $4f$ magnetic moments of the Pr^{3+} ions with the applied magnetic field $\mathbf{H}$ and the third term is the mean-field approximation of an isotropic bilinear Heisenberg-type interaction, where $\mathbf{H}_{\mathrm{ex}}(j)$ is the exchange field acting on ion j. The fourth term is a corrective energy term due to the mean-field treatment. Due to the periodicity represented through the propagation vector $\mathbf{k}$ of the incommensurate magnetic structure, the magnetic moment $\mathbf{M}(j)$ and the exchange field $\mathbf{H}_{ex}(j)=(g_J\mu_B)^{-2}\Sigma_{i\neq j}J(ij)\langle\mathbf{M}(i)\rangle$ can be expanded in Fourier series

$$\mathbf{M}(j) = \sum_n \mathbf{M}_{n\mathbf{k}}e^{in\mathbf{k}\cdot\mathbf{R}_j}, \qquad (3)$$

$$\mathbf{H}_{ex}(j) = \frac{1}{(g_J\mu_B)^2}\sum_n J(n\mathbf{k})\mathbf{M}_{n\mathbf{k}}e^{in\mathbf{k}\cdot\mathbf{R}_j}. \qquad (4)$$

From a self-consistent diagonalization of the Hamiltonian (2), using $N=16$ and an effective propagation vector $\mathbf{k}_{\mathrm{eff}}=(0,0,0.87/2)\approx(0,0,7/16)$ (owing to the body-centered crystal structure), the Fourier coefficients $\mathbf{M}_{n\mathbf{k}}$ calculated after diagonalization are reinjected into the Hamiltonian through Eq. (4) until self-consistency is attained. From this procedure the temperature and magnetic field dependence of the $\mathbf{M}_{n\mathbf{k}}$ can be calculated.

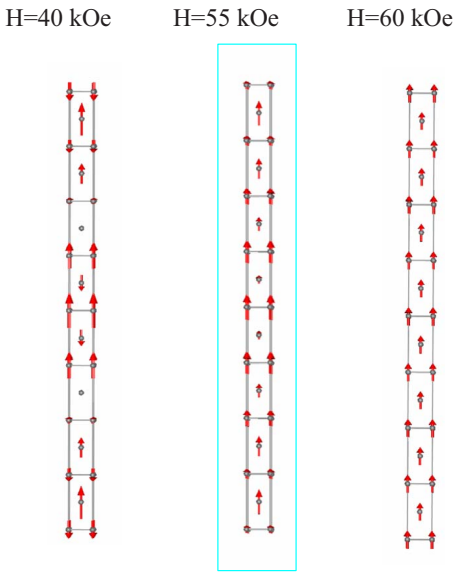

FIG. 7. (Color online) Schematic projection of the magnetic structure of $PrNi_2Si_2$ on the *ac* plane of the body-centered tetragonal unit cell for fields $H \| c$ of (a) 40, (b) 55, and (c) 60 kOe, respectively. The three arrangements are characteristics of the three regions that can be found depending on the relative magnitude between $M_{\mathbf{k}}$ and M_0 (see text). The blue box corresponds to the blue shadowed area in Fig. 6.

The magnetic properties of $PrNi_2Si_2$ are well accounted for by this model, using the above crystal-field parameters and two parameters for the Fourier transform $J(\mathbf{q})$ of the exchange interactions, namely, $J(\mathbf{q}=0)=-0.21$ K and $J(\mathbf{q}=\mathbf{k})=2.27$ K. Note that we have not adjusted any of these parameters in the present calculations but use the original parameter set of Blanco *et al.*[12,13] The calculated values of the zero-temperature Fourier components, $M_{\mathbf{k}}=2.26$ and $M_{3\mathbf{k}}=0.25\ \mu_B$, are in excellent agreement with the observed values, 2.35(2) and 0.34(19) μ_B, respectively. The ground state corresponding to the (maximum) moment of 2.26 μ_B is obtained from a diagonalization of Eq. (2) and is given by

$$|\Psi\rangle = 0.87|-4\rangle + 0.44|0\rangle + 0.22|4\rangle \approx 0.92|\Gamma_1^{(1)}\rangle - 0.47|\Gamma_2\rangle.$$

The molecular magnetic field for this particular ion reaches values as large as ~150 kOe leading to a total exchange mean-field energy of ~25 K, which is comparable to the gap between the crystal-field ground state and the first excited singlet state (see above).

The calculated *temperature dependence* at zero applied magnetic field of both the first and third harmonics are in good agreement with the experimental results, as shown in Fig. 4. The inset of the figure shows the temperature dependence of the ratio $M_{3\mathbf{k}}/M_{\mathbf{k}}$. The experimental observation that the third harmonic decreases faster with temperature than the first harmonic to give a perfect sine-modulated structure close to T_N is qualitatively reproduced by the periodic field model.

The *field dependence* $H \| c$ of the magnetic structure is also predicted by the periodic field model, via the second term in Eq. (2). Using the MCPHASE program package,[22] we calculated the Fourier component $M_{\mathbf{k}}$ [Fig. 6(a)] and the induced ferromagnetic component M_0 [Fig. 6(b)] as a function of field. The agreement between calculated and experimental data is satisfactory. The results obtained from the McPhase program allow us to define three regions depending on the relative magnitude of $M_{\mathbf{k}}$ and M_0, as illustrated in Fig. 7. (i) For $M_0 < M_{\mathbf{k}}$ the magnetic structure has the modulated character found at zero field, where some magnetic moments at particular sites through the magnetic period are antiparallel to the applied magnetic field [shown at $H=40$ kOe in Fig. 7(a)]. (ii) For $0 < M_{\mathbf{k}} < M_0$ all the magnetic moments are parallel to the applied magnetic field but with a residual modulation [shown at $H=55$ kOe in Fig. 7(b)]. This is the situation within the blue shadowed region of Fig. 6, at 5–6 kOe below the cusp in the magnetization observed at $H=58$ kOe. (iii) Above $H=58$ kOe, $M_{\mathbf{k}}=0$ and the induced full ferromagnetic arrangement is reached [shown at $H=60$ kOe in Fig. 7(c)]. Note that the magnetic moment of $M_0=1.3\ \mu_B$ at 60 kOe is not yet saturated due to crystal field effects.

The calculated critical field, above which the moments align ferromagnetically along the applied field direction, is $H_c=60$ kOe for $H \| c$. This prediction is in good agreement with the experimental value of 58 kOe as observed in both the present neutron scattering experiment and in magnetization measurements.[12,13]

V. CONCLUSION

Using single-crystal neutron diffraction, we have shown that the amplitude-modulated magnetic structure that develops below $T_N=20$ K in $PrNi_2Si_2$ remains essentially sinusoidal down to the lowest temperatures, with only a very weak third harmonic, $m_{3\mathbf{k}}/m_{\mathbf{k}} \sim 1/7$, at $T=1.6$ K. This is consistent with an easy-axis anisotropy and a singlet crystal-field ground state, where the magnetic moment is induced by the RKKY exchange interaction, which mixes the ground-state singlet with the first excited singlet.

We also found that the intensity of the first harmonic decreases when a magnetic field is applied along the easy axis and it disappears at a critical field of $H_c=58$ kOe. The induced ferromagnetic moment increases with increasing magnetic field, and shows a kink at H_c, where the amplitude modulated structure becomes aligned ferromagnetically along the applied field. This is in good agreement with magnetization measurements.

These results are well described with a self-consistent periodic mean-field model, where the five crystal-field parameters were obtained from a joint analysis of specific-heat, magnetization, magnetic-susceptibility, and inelastic neutron-scattering measurements.[12–15] The exchange interaction was modeled using two parameters for $J(\mathbf{q})$, at $\mathbf{q}=0$ and $\mathbf{k}$. The model reproduces the crystal-field scheme, the macroscopic properties, the temperature and magnetic field dependence of the first harmonic, the field dependence of the induced ferromagnetic moment, and the critical field H_c where ferromagnetic order is established.

ACKNOWLEDGMENTS

Financial support has been received from Spanish MEC and FEDER Grant No. MAT2008-06542-C04-03. Technical support from P. Fouilloux and S. Capelli is acknowledged. We also thank SpINS for beam time allocation on the CRG D15.

[1] A. P. Ramirez, Annu. Rev. Mater. Sci. **24**, 453 (1994).
[2] A. P. Ramirez, Nature (London) **421**, 483 (2003).
[3] E. A. Goremychkin, R. Osborn, B. D. Macaluso, D. T. Adroja, and M. Koza, Nat. Phys. **4**, 766 (2008).
[4] A. Szytula and L. Leciejewicz, in *Handbook on the Physics and Chemistry of Rare Earths*, edited by K. A. Gschneidner, Jr. and L. Eyring (Elsevier Science, Amsterdam, 1989), Chap. 83.
[5] O. Moze, in *Handbook of Magnetic Materials*, edited by K. H. J. Buschow (Elsevier, Amsterdam, 1998), Chap. 4, p. 493.
[6] J. Rossat-Mignod, in *Methods in Experimental Physics*, edited by K. Sköld and D. L. Price (Academic Press, Amsterdam, 1987), Vol. 23C, p. 131.
[7] G. Shirane and W. J. Takei, J. Phys. Soc. Jpn. **17**, Suppl. B-III, 35 (1962).
[8] W. C. Koehler, in *Magnetic Properties of Rare Earths Metals*, edited by R. J. Elliot (Plenum, New York, 1972), Chap. 3, p. 81.
[9] T. Chattopadhyay, P. J. Brown, and H. G. von Schnering, Phys. Rev. B **36**, 7300 (1987).
[10] J. M. Barandiarán, D. Gignoux, D. Schmitt, and J. C. Gómez-Sal, Solid State Commun. **57**, 941 (1986).
[11] J. A. Blanco, D. Gignoux, J. C. Gómez-Sal, and D. Schmitt, J. Magn. Magn. Mater. **104-107**, 1273 (1992).
[12] J. A. Blanco, D. Gignoux, and D. Schmitt, Phys. Rev. B **45**, 2529 (1992).
[13] J. A. Blanco, D. Schmitt, and J. C. Gómez-Sal, J. Magn. Magn. Mater. **116**, 128 (1992).
[14] J. A. Blanco, R. M. Nicklow, and D. Schmitt, Physica B **213-214**, 327 (1995).
[15] J. A. Blanco, R. M. Nicklow, and D. Schmitt, Phys. Rev. B **56**, 11666 (1997).
[16] J. A. Blanco, B. Fåk, R. M. Nicklow, B. Roessli, and D. Schmitt, Physica B **234-236**, 756 (1997).
[17] P. J. Brown, in *International Tables for Crystallography*, edited by E. Prince (The International Union of Crystallography, Boston, 2004), Chap. 4.4.5, p. 454.
[18] M. Rotter and A. T. Boothroyd, Phys. Rev. B **79**, 140405(R) (2009).
[19] J. H. van Vleck, *The Theory of Electric and Magnetic Susceptibilities* (Oxford University Press, London, 1932), Chap. 9.
[20] M. T. Hutchings, Solid State Phys. **16**, 227 (1964).
[21] A. M. Mulders, A. Yaouanc, P. Dalmas de Réotier, P. C. M. Gubbens, A. A. Moolenaar, B. Fåk, E. Ressouche, K. Prokeš, A. A. Menovsky, and K. H. J. Buschow, Phys. Rev. B **56**, 8752 (1997).
[22] M. Rotter, J. Magn. Magn. Mater. **272-276**, E481 (2004).